Detection of the simplest sugar, glycolaldehyde, in a solar-type protostar with ALMA

Jes K. Jørgensen[1,2], Cécile Favre[3], Suzanne E. Bisschop[2,1], Tyler L. Bourke[4], Ewine F. van Dishoeck[5,6], and Markus Schmalzl[5]

ABSTRACT

Glycolaldehyde ($HCOCH_2OH$) is the simplest sugar and an important intermediate in the path toward forming more complex biologically relevant molecules. In this paper we present the first detection of 13 transitions of glycolaldehyde around a solar-type young star, through Atacama Large Millimeter Array (ALMA) observations of the Class 0 protostellar binary IRAS 16293-2422 at 220 GHz (6 transitions) and 690 GHz (7 transitions). The glycolaldehyde lines have their origin in warm (200–300 K) gas close to the individual components of the binary. Glycolaldehyde co-exists with its isomer, methyl formate ($HCOOCH_3$), which is a factor 10–15 more abundant toward the two sources. The data also show a tentative detection of ethylene glycol, the reduced alcohol of glycolaldehyde. In the 690 GHz data, the seven transitions predicted to have the highest optical depths based on modeling of the 220 GHz lines all show red-shifted absorption profiles toward one of the components in the binary (IRAS16293B) indicative of infall and emission at the systemic velocity offset from this by about $0.2''$ (25 AU). We discuss the constraints on the chemical formation of glycolaldehyde and other organic species – in particular, in the context of laboratory experiments of photochemistry of methanol-containing ices. The relative abundances appear to be consistent with UV photochemistry of a CH_3OH–CO mixed ice that has undergone mild heating. The order of magnitude increase in line density in these early ALMA data illustrate its huge potential to reveal the full chemical complexity associated with the formation of solar system analogs.

Subject headings: astrochemistry — astrobiology — stars: formation — ISM: abundances — ISM: molecules — ISM: individual (IRAS 16293-2422)

[1]Centre for Star and Planet Formation and Niels Bohr Institute, University of Copenhagen, Juliane Maries Vej 30, DK-2100 Copenhagen Ø., Denmark, jeskj@nbi.dk

[2]Centre for Star and Planet Formation and Natural History Museum of Denmark, University of Copenhagen, Øster Voldgade 5–7, DK-1350 Copenhagen K., Denmark, suzanne@snm.ku.dk

[3]Department of Physics and Astronomy, Aarhus University, Ny Munkegade, DK-8000, Aarhus C., Denmark, favre@phys.au.dk

[4]Harvard-Smithsonian Center for Astrophysics, 60 Garden Street, Cambridge, MA 02138, USA, tbourke@cfa.harvard.edu

[5]Leiden Observatory, Leiden University, PO Box 9513, NL-2300 RA Leiden, The Netherlands, ewine@strw.leidenuniv.nl, schmalzl@strw.leidenuniv.nl

[6]Max-Planck Institut für extraterrestrische Physik, Giessenbachstrasse, D-85748 Garching, Germany

1. Introduction

One of the most intriguing questions in studies of the chemistry of the early solar system is whether, how, when and where complex organic and potentially prebiotic molecules are formed. One of the key species in this context is glycolaldehyde (HCOCH$_2$OH). It is the simplest sugar and the first intermediate product in the formose reaction that begins with formaldehyde (H$_2$CO) and leads to the (catalyzed) formation of sugars and ultimately ribose, the backbone of RNA, under early Earth conditions (e.g., Larralde et al. 1995). The presence of glycolaldehyde is therefore an important indication that the processes leading to biologically relevant molecules are taking place. However, the mechanism responsible for its formation in space is still unclear (see, e.g., Woods et al. 2012).

Glycolaldehyde has so-far been detected in two places in space – toward the Galactic center source SgrB2(N) (Hollis et al. 2000; see also Hollis et al. 2001; Hollis et al. 2004; Halfen et al. 2006; Requena-Torres et al. 2008) and the high-mass hot molecular core G31.41+0.31 (Beltrán et al. 2009). Another compelling related discovery is that of ethylene glycol ("anti-freeze"; (CH$_2$OH)$_2$), the reduced alcohol variant of glycolaldehyde, found also toward SgrB2(N) at comparable abundances (Hollis et al. 2002). Searches for glycolaldehyde in comets have so-far only resulted in upper limits, whereas ethylene glycol is detected toward Hale-Bopp and found to be at least 5 times more abundant than glycolaldehyde (Crovisier et al. 2004). Comparisons between these species are therefore particularly interesting as their relative abundances potentially provide strong constraints on their formation and the chemical evolution from protostars to primitive solar system material.

The protostellar (Class 0) binary IRAS16293-2422 (IRAS16293 hereafter) at a distance of 120 pc (Loinard et al. 2008) has long been considered to be the best low-mass protostellar testbed for astrochemical studies (see, e.g., Blake et al. 1994; van Dishoeck et al. 1995; Ceccarelli et al. 2000; Schöier et al. 2002), a status that has been further bolstered by the detection of a wealth complex organic molecules toward this source (Cazaux et al. 2003; Caux et al. 2011). (Sub)millimeter wavelength interferometric studies of its chemistry have revealed strong differentiation among different species toward the two components in the binary (IRAS16293A and IRAS16293B; Wootten 1989) including complex organic molecules (Bottinelli et al. 2004; Schöier et al. 2004; Bisschop et al. 2008; Jørgensen et al. 2011).

With the Atacama Large Millimeter/submillimeter Array (ALMA) beginning operations a completely new opportunity has arisen for studies of the astrochemistry of solar-type stars. ALMA provides high sensitivity for faint lines, high spectral resolution which limits line confusion, and high angular resolution making it possible to study young stars on solar-system scales. In this letter we report the first potential discoveries of glycolaldehyde and ethylene glycol in a solar-type protostar from ALMA observations of IRAS 16293-2422.

2. Observations

IRAS 16293-2422 was observed on 2011 August 16–17 as part of the ALMA Science Verification (SV) program in band 6 (see also Pineda et al. 2012). At the time of observations 16 antennae were present in the array in a compact configuration resulting in a synthesized beam size of $2.5'' \times 1.0''$ (PA = 92°). The source was observed in a two-point mosaic with a total integration time of 5.5 hrs. The observations contain one spectral window with 3840 channels and a channel width of 61.0 kHz (0.083 km s^{-1}) covering a bandwidth from 220.078 GHz to 220.313 GHz. The resulting line RMS noise level is estimated to be 13 mJy beam^{-1} channel^{-1} in off-source line free channels.

IRAS 16293-2422 was further observed in ALMA's band 9 on 2012 April 16–17 with 13 antennae in the array. For these observations a seven-point mosaic was performed with the array in an extended configuration resulting in a synthesized beam size of $0.29'' \times 0.18''$ (PA = 113°) covering the full spectral ranges 686.5–692.2 GHz (except 688.35-688.50 GHz) and 703.2–705.1 GHz with an effective spectral resolution of 980 kHz (0.4 km s^{-1}). In total about 9.2 hrs were spent on the mosaic resulting in an RMS of 0.11 Jy beam^{-1} channel^{-1}.

For both datasets we followed the reduction in the CASA cookbooks/scripts delivered together with the SV data. To test the reliability of the SV data we compared the resulting band 6 spectra to our large Submillimeter Array survey (SMA, Jørgensen et al. 2011; Bisschop et al. 2008). Excellent agreement is seen between the SMA and ALMA spectra at the two continuum peaks with fluxes for bright lines agreeing to better than 10–20%. This illustrates that the relative calibration of the two arrays is good but also, equally important, that the detected line emission is compact in both beams: the larger SMA beam of $4'' \times 2.4''$ does not pick up significant extended emission that may have been missed by ALMA.

3. Results

Fig. 1 shows the band 6 spectra at 220.2 GHz within one synthesised beam toward the two continuum peaks marking the locations of IRAS16293A (α=16$^{\rm h}$32$^{\rm m}$22.87$^{\rm s}$; δ=−24$^{\rm d}$28′36′′39) and IRAS16293B (α=16$^{\rm h}$32$^{\rm m}$22.62$^{\rm s}$; δ=−24$^{\rm d}$28′32′′46). A large number of lines are clearly seen toward both positions. The widths of the lines follow the pattern seen in previous studies, with IRAS16293A showing lines about a factor of 5 broader than those toward IRAS16293B. Also, as seen in previous observations (e.g., Bottinelli et al. 2004) many of the lines toward IRAS16293B show red-shifted absorption features against the continuum indicative of infalling motions.

In the 220 GHz data the most easily identifiable species is methyl formate, which is responsible for the two brightest lines at 220.1669 and 220.1903 GHz as well as a handful of other lines. A number of other species are easily detected, including ketene (CH_2CO) at 220.1776 GHz and trans-ethanol (t-C_2H_5OH) at 220.1548 GHz (see also Bisschop et al. 2008). More remarkable is a set of clearly detected lines that can be attributed to glycolaldehyde. Table 1 lists the identified transitions of methyl formate and glycolaldehyde, including lines in vibrationally excited levels, together with references to the laboratory spectroscopy data
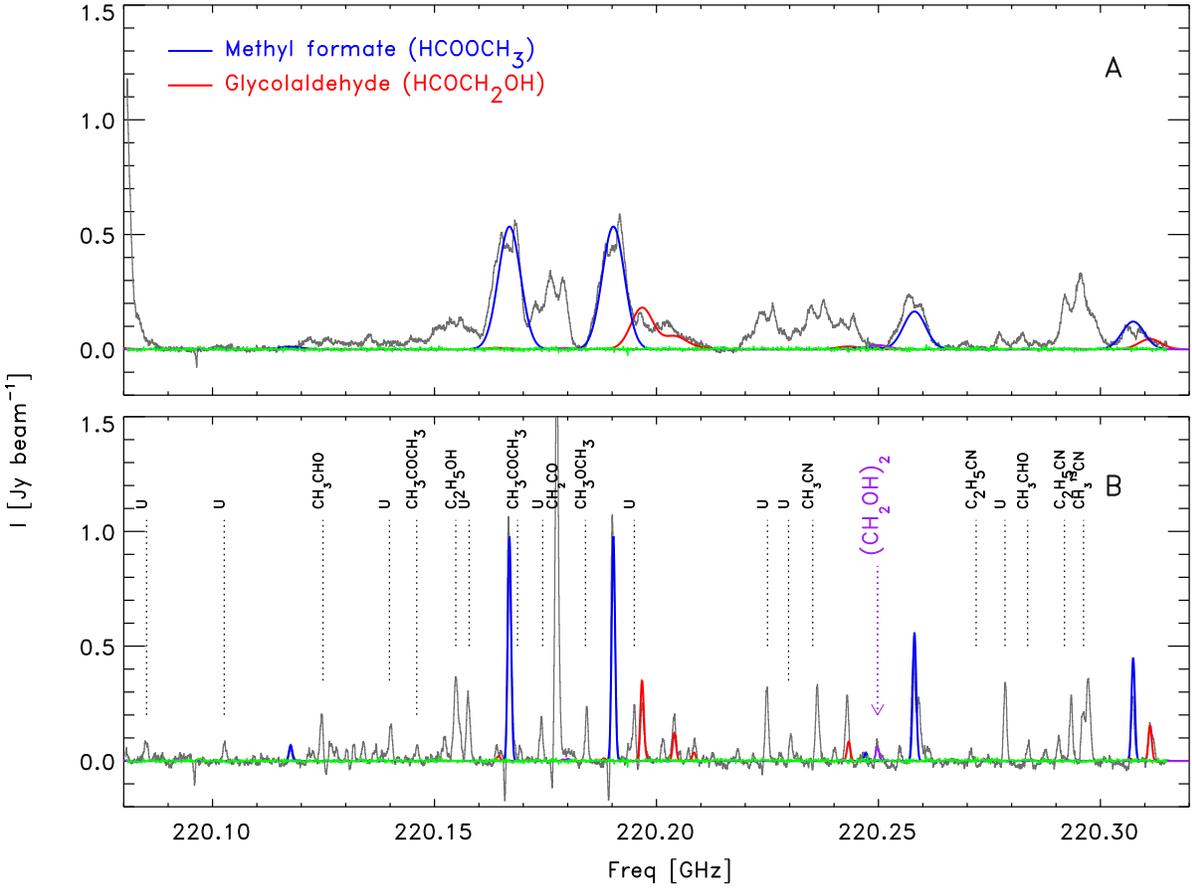
Fig. 1.— Spectra in the central beams toward the continuum peaks of IRAS16293A (upper) and IRAS16293B (lower). Fits from LTE models of the methyl formate (blue) and glycolaldehyde (red) emission are overplotted. The purple line indicates the model fit to the possible ethylene glycol transition. The X-axis represents the frequencies in the rest frame of the system (i.e., corrected for the system V_{LSR} of 3 km s^{-1}). The green line is an indication of the RMS level (13 mJy beam^{-1}) represented by a spectrum extracted from an off source position. Note the much narrower lines toward IRAS16293B which facilitate identification of individual features.

– 5 –

on which the frequencies are based. Simultaneous Gaussian fits to all lines in the central beams toward each of the sources were made to determine line intensities. For IRAS16293A the average width of all lines from the Gaussian fits is 6.3 km s^{-1} while for IRAS16293B it is 1.4±0.3 km s^{-1}, indicating very small differences in widths between the lines. Likewise the average V_{LSR} is 3.0 km s^{-1} for IRAS16293A and 2.7 km s^{-1} for IRAS16293B with standard deviations of only 0.1–0.2 km s^{-1}. For comparison the quoted uncertainties for the predicted line rest frequencies correspond to 0.01–0.02 km s^{-1}. The systemic velocities and line widths are in good agreement with the large set of lines detected with the SMA (Jørgensen et al. 2011). All lines of methyl formate and glycolaldehyde have similar spatial extents toward each of the two sources. Fig. 2 shows close-ups of each identified glycolaldehyde line toward IRAS16293B at 220 GHz.

To further validate the detections of the methyl formate and glycolaldehyde lines, we modeled the strengths for all their lines in the observed band assuming an isothermal medium and LTE excitation and taking into account the optical thickness of the lines (see, e.g., Goldsmith et al. 1999). Fig. 1 includes the best fit models to the methyl formate and glycolaldehyde lines. The fits show comparable temperatures for the two species (200 and 300 K for IRAS16293A and IRAS16293B, respectively). The derived column densities averaged over 0.5″ (60 AU) regions are given in Table 2. The model reproduces the observed line profiles and strengths very well, including the vibrationally excited lines, even for this fairly simplified model.

The 220 GHz data also show a tentative detection of ethylene glycol. The strongest line of ethylene glycol ($22_{2,20}$ ($v = 1$) − $21_{2,19}$ ($v = 0$) at 220.2498 GHz; $E_u = 127$ K) in the band coincides with a ≈18σ line toward IRAS16293B that is difficult to attribute to any other species. Using the LTE model at 300 K, the observed line strength would require an ethylene glycol abundance of 0.3–0.5 with respect to glycolaldehyde. This is comparable to the estimates by Hollis et al. (2002) for SgrB2(N), but notably smaller than the inferred values from comet Hale-Bopp where ethylene glycol is at least five times more abundant than glycolaldehyde (Crovisier et al. 2004).

Similar model calculations can rule out some of the alternative identifications for the lines ascribed to glycolaldehyde. Cyclopropenylidene (c-C$_3$H$_2$) for example has two transitions at 220.2025 GHz that potentially could be confused with the glycolaldehyde line at 220.2040 GHz. However, these specific transitions of c-C$_3$H$_2$ have very low Einstein A coefficients (∼ 10^{-8} s^{-1}), so that for any reasonable excitation temperature, other stronger lines of this species should have been observed in the frequency range covered by the SMA observations – e.g., between 230.5 and 231.0 GHz[1]. Also, if ascribed to c-C$_3$H$_2$, this emission would be red-shifted by about 2 km s^{-1} which should be easily discernable toward IRAS16293B. Likewise the transitions at 220.196 GHz could also be attributed to a vinyl cyanide (CH$_2$CHCN) line at 220.1964 GHz. However, this species would have a much stronger transition at 220.138 GHz that is not seen.

A strong confirmation of the identification of glycolaldehyde is provided by the 690 GHz observations. A large number of glycolaldehyde transitions are expected to be located in this band with a range of energy

[1]Lines of this species detected previously using single-dish observations have significantly higher Einstein A coefficients, ∼10^{-4}–10^{-3} s^{-1}, and are likely somewhat extended.

Table 1: Identified lines and results from Gaussian fit to emission.

Molecule	Transition	Frequency [GHz]	$\log_{10} A_{ul}$ [s^{-1}]	E_u [K]	Flux [Jy km s^{-1}][a] I_A	I_B	$V_{LSR,B}$[c] [km s^{-1}]
		Band 6 lines					
HCOOCH$_3$	$33_{9,25} - 33_{8,26}$A $v_t = 1$	220.1176	−4.18	572.6	0.14	0.063	2.5
	$17_{4,13} - 16_{4,12}$E $v_t = 0$	220.1669	−3.82	103.2	4.36	1.39	2.6
	$17_{4,13} - 16_{4,12}$A $v_t = 0$	220.1903	−3.82	103.1	4.16	1.43	2.6
	$24_{1,23} - 24_{0,24}$E $v_t = 1$	220.2472	−5.46	355.1	0.056	0.061	2.9
	$18_{8,10} - 17_{8,9}$E $v_t = 1$	220.2581[b]	−3.89	330.8	1.89	0.66	2.7
	$24_{2,23} - 24_{1,24}$E $v_t = 1$	220.2585[b]	−5.46	355.1	. . .	. . .	. . .
	$18_{10,9} - 17_{10,8}$E $v_t = 1$	220.3074	−3.95	354.3	0.69	0.38	2.6
HCOCH$_2$OH	$11_{3,8} - 10_{2,9}$ $v = 1$	220.1644	−4.37	323.5	. . .	0.092	2.9
	$7_{6,2} - 6_{5,1}$ $v = 0$	220.1966[b]	−3.60	37.4	1.04	0.34	2.8
	$7_{6,1} - 6_{5,2}$ $v = 0$	220.1968[b]	−3.60	37.4	. . .	. . .	. . .
	$11_{4,7} - 10_{3,8}$ $v = 0$	220.2040	−3.99	46.6	0.83	0.28	2.6
	$11_{4,7} - 10_{3,8}$ $v = 2$	220.2084	−3.98	420.8	0.12	0.13	2.4
	$36_{10,27} - 36_{9,28}$ $v = 1$	220.2433	−3.69	713.0	1.14	0.38	2.9
	$7_{6,2} - 6_{5,1}$ $v = 1$	220.3111[b]	−3.60	318.2	0.25	0.26	2.5
	$7_{6,1} - 6_{5,2}$ $v = 1$	220.3113[b]	−3.60	318.2	. . .	. . .	. . .
		Band 9 lines[d]					
HCOCH$_2$OH	$38_{11,28} - 37_{10,27}$ $v = 0$	686.6517	−2.53	488.1	. . .	. . .	. . .
	$30_{14,16/17} - 29_{13,17/16}$ $v = 0$	687.0513	−2.30	377.4	. . .	. . .	. . .
	$19_{19,0/1} - 18_{18,1/0}$ $v = 0$	687.4445	−1.99	324.6	. . .	. . .	. . .
	$35_{12,24} - 34_{14,23}$ $v = 0$	689.4295	−2.42	438.8	. . .	. . .	. . .
	$35_{12,23} - 34_{14,24}$ $v = 0$	689.5776	−2.42	438.8	. . .	. . .	. . .
	$28_{15,13/14} - 27_{14,14/13}$ $v = 0$	689.8903	−2.24	362.1	. . .	. . .	. . .
	$27_{16,11/12} - 26_{15,12/11}$ $v = 0$	703.8607	−2.17	365.3	. . .	. . .	. . .
	$42_{11,32} - 41_{10,31}$ $v = 0$[e]	704.8369	−2.57	580.0	. . .	. . .	. . .

Notes: Molecular data are taken from the JPL and CDMS catalogs (Pickett et al. 1998; Müller et al. 2001, 2005). The glycolaldehyde molecular data are based on laboratory measurements by Butler et al. (2001), Widicus Weaver et al. (2005) and Caroll et al. (2010) and model predictions based on these (see text) as provided by the JPL June 2012 catalog entry. [a]Total flux from Gaussian fits to the line emission in the central beam toward IRAS16293A (I_A) and IRAS16293B (I_B). For conversion to brightness temperatures, the gain of the interferometric observations with the given beam size is 0.1 Jy K^{-1}. [b]Transitions not resolved. [c]V_{LSR} toward IRAS16293B. [d]Lines show emission off-source and red-shifted absorption on-source. [e]Shown in Fig. 3; not detected.
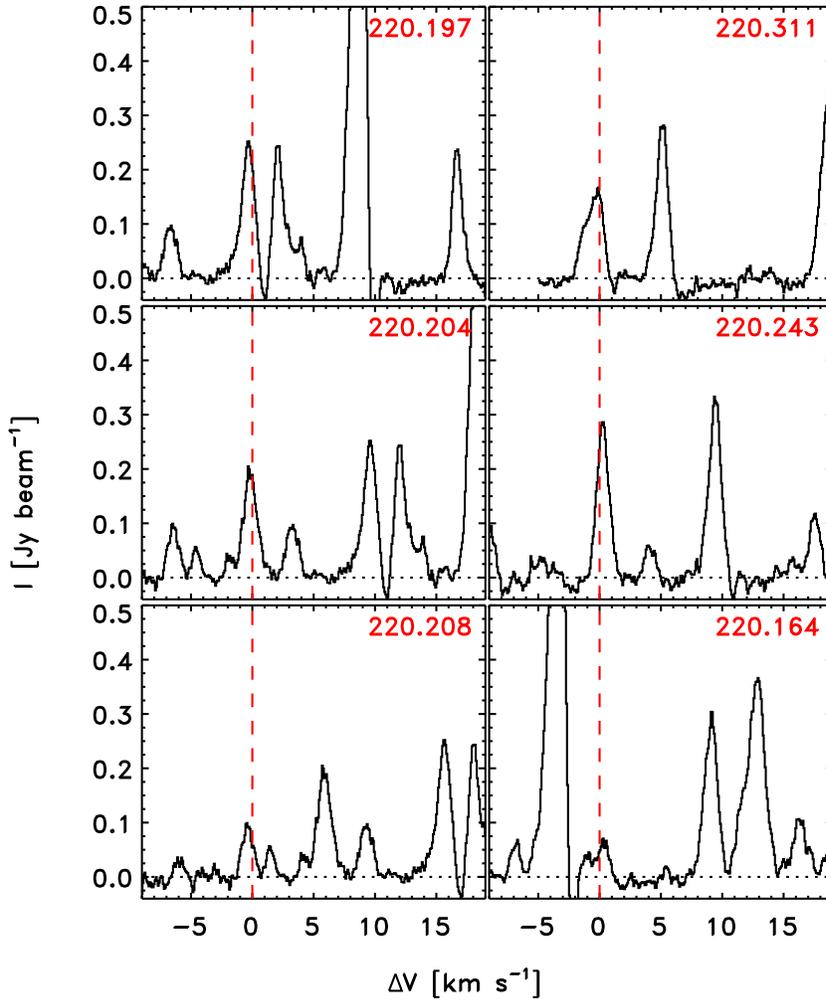
Fig. 2.— Zoom-in on the glycolaldehyde transitions detected at 220 GHz. The velocities on the X-axis is given relative to the systemic velocity of 2.7 km s^{-1}.
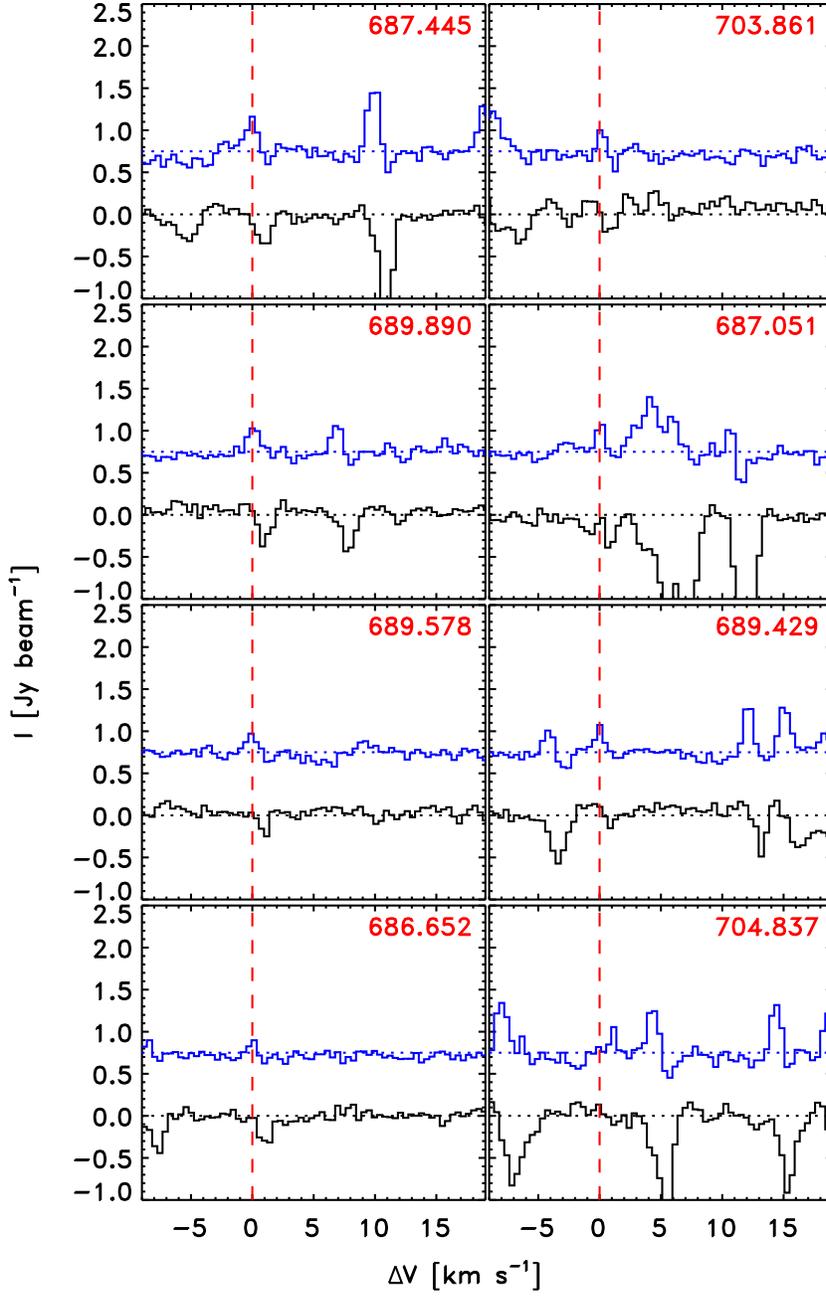
Fig. 3.— Zoom-in on the glycolaldehyde transitions predicted to be most optically thick at 690 GHz toward the IRAS16293B continuum peak (*black*) and toward a position offset by one synthesized beam from the continuum peak (*blue*; shifted by 0.75 Jy beam^{-1} in the Y-axis direction). As in Fig. 2 the velocities on the X-axis is given relative to the systemic velocity.

levels and line strengths. The model based on the 220 GHz data predicts that a number of these transitions are becoming optically thick ($\tau_{60 \text{ AU}} \gtrsim 0.1 - 1.0$ averaged over the 0.5″ region used for the column density estimates). Fig. 3 shows the spectra toward the IRAS16293B continuum peak as well as offset by one synthesized beam for the lines expected to be most optically thick. Toward the continuum peak, the 7 most optically thick transitions all show red-shifted absorption against the IRAS16293B continuum whereas they are seen in emission at the offset position. Again, these lines show a nearly perfect correspondance to the expected systemic velocity of 2.7 km s^{-1}. Equally important, the models do not predict other lines of glycolaldehyde that should be detectable elsewhere in the large 690 GHz spectral window at the sensitivity of the observations, nor in the 220 GHz window. The absence of emission toward the continuum peak for IRAS16293B suggests that the continuum is completely optically thick at these high frequencies and scales (0.25″; 30 AU diameter). This is consistent with the observations of Chandler et al. (2005) who showed that the continuum at centimeter wavelengths was due to optically thick thermal dust emission at the same scales (0.15–0.25″). The fact that glycolaldehyde and other complex species show infall signatures toward source B (see also Pineda et al. 2012) implies that these molecules are moving toward the planet-forming zones at $\leq$ 30 AU radius.

The main uncertainty in the assignments is the accuracy and completeness of the spectroscopic catalogs. About one third of the lines brighter than about 0.1 Jy beam^{-1} remain unidentified in the 220 GHz spectrum and other possible assignments for the potential glycolaldehyde lines can thus not be ruled out. Also, not all glycolaldehyde line frequencies have been measured directly in the laboratory, especially for the vibrationally excited states detected here and for the lines at 690 GHz, but are based on a spectroscopic model using measurements at other frequencies. However, since the laboratory data cover lines up to 1.2 THz and include other vibrationally excited lines with a similar range of J and K_a values as observed here, the frequency predictions should be reliable. Indeed, their quoted uncertainties are lower than what can be discerned in our data. A check can be made by comparing the frequencies from the JPL and CDMS catalogs which have been computed using slightly different methods and datasets. For the lines detected in the ALMA spectra, the agreement between the frequencies is about 0.2 MHz – corresponding to < 0.1 km s^{-1}. Thus, within the uncertainties given in the catalogs the identification of lines are secure. Also, the relative column density (or abundance) of methyl formate to glycolaldehyde of 10–15 is consistent with previous measurements (see also § 4) and, combined with the additional high frequency detections and the close matches in velocity for 13 lines, provide a compelling case for the assignments. We stress that IRAS16293B with its narrow line widths provides a much cleaner source for identification of complex species than high mass sources like SgrB2(N) that have been studied so far. Future searches with ALMA will be able to further strengthen the assignments either by extending the number of lines or searching for specific spectroscopic signatures – e.g., those provided by the low excitation $v = 0$ transitions used for previous detections at 3 mm.

4. Discussion: formation of glycolaldehyde

The similar spectral shapes of the lines of the complex organic molecules (in particular, the line widths and the absorption profiles toward IRAS16293B) as well as their similar spatial extent suggest that methyl

formate, glycolaldehyde and other species coexist in the same gas. Furthermore, methyl formate and glycolaldehyde are fit by similar excitation temperatures in our simple LTE models. Therefore, a discussion of the chemical relation between glycolaldehyde and methyl formate is relevant.

Our results indicate that methyl formate is a factor 10–15 more abundant than glycolaldehyde in the warm gas toward the two binary components of IRAS16293-2422. This value is consistent with previous measurements ranging from 52 in the hot core of SgrB2(N) (Hollis et al. 2001) and the upper limit of 34 in G34.41+0.31 (Beltrán et al. 2009) to the average of 5–6.5 found on more extended scales toward SgrB2(N) (Hollis et al. 2000; Requena-Torres et al. 2008). Relative to the lower limit on the H_2 column density from the optically thick dust continuum emission toward IRAS16293B (Chandler et al. 2005) and taking into account the filling factor, the two species are estimated to have abundances relative to H_2 of 8×10^{-8} (methyl formate) and 6×10^{-9} (glycolaldehyde).

One of the major discussions concerning the origin of complex organic molecules in space is whether these form from second generation gas-phase reactions based on protonated CH_3OH (released from ices at high temperatures) or due to first generation reactions in the icy grain mantles, possibly induced by UV- or cosmic-ray irradiation (e.g., Herbst & van Dishoeck 2009). Grain-surface reactions are becoming increasingly more popular, especially since the formation of methyl formate through gas-phase reactions seems to be too inefficient to explain the observed abundances (Horn et al. 2004).

Halfen et al. (2006) compared a survey of the glycolaldehyde emission toward SgrB2(N) with formaldehyde (H_2CO), motivated by the first step in the formose reaction consisting of two H_2CO molecules combining to form $HCOCH_2OH$. Modeling the emission from $H_2C^{18}O$ transitions detected in our SMA survey with the same excitation temperature as for methyl formate and glycolaldehyde suggests a formaldehyde to glycolaldehyde abundance ratio of 42–56 (using a $^{16}O:^{18}O$ abundance ratio of 560 characteristic for the local ISM (Wilson & Rood 1994)). This is in agreement with the estimate by Halfen et al. (2006) of a ratio of 27 in SgrB2(N). Halfen et al. interpreted this ratio in favor of the formation of glycolaldehyde in space through a gas-phase formose reaction. However, as pointed out by Woods et al. (2012) this and other gas-phase reactions tend to produce too little glycolaldehyde compared to observed abundances in an absolute sense.

Alternatively glycolaldehyde may be formed through grain-surface reactions in ices rich in methanol (CH_3OH) or its derivatives. From laboratory experiments Öberg et al. (2009) found that photochemistry of UV-irradiated methanol ices mixed with significant amounts of CO can explain the observed fractions of oxygen-rich complex organics like methyl formate relative to methanol in sources such as IRAS16293 (Bisschop et al. 2008). Although Öberg et al. (2009) could not fully separate glycolaldehyde and methyl formate in their methanol-rich experiments, the derived lower limits on their abundances in CO-containing ices relative to methanol are 4% and 8%, respectively, consistent with the combined IRAS16293 results of Bisschop et al. (2008) and those found here of $\approx$ 1% and 10–20%. Also, their upper limit of ethylene glycol relative to glycolaldehyde (<25%) agrees roughly with our ratio of 0.3–0.5. Experiments with irradiation of pure CH_3OH ices on the other hand produce too large ethylene glycol abundances relative to glycolaldehyde by an order of magnitude. The CH_3OH:CO ratio is clearly critical: laboratory results for the CH_3OH:CO=1:10

mixtures show a 4 times larger abundance of glycolaldehyde relative to ethanol, whereas the ethanol lines detected here and in the previous SMA observations (Bisschop et al. 2008) suggests that ethanol is 3–5 times more abundant than glycolaldehyde in IRAS16293. As pointed out by Öberg et al. (2009) the relative abundances of some species also strongly depend on the ice temperature, with the glycolaldehyde and ethylene glycol production requiring heating above ~30 K. Thus, both exact ice composition (amount of CO mixed with CH_3OH) and temperature play a role in the chemistry; a combination of a moderately CO-rich ice and mild heating best reproduce the current data.

Still, additional systematic surveys of more species and sources are needed to constrain the surface formation mechanisms in more detail. These early data illustrate the enormous potential of ALMA for doing this. The current sensitivity is already more than an order of magnitude better than that of previous single-dish or interferometric line surveys toward this source (Caux et al. 2011; Jørgensen et al. 2011), revealing a line density toward IRAS16293B nearly ten times higher than before. Clearly, ALMA is posed to reveal many more complex organic molecules in young solar-system analogs.

REFERENCES

Beltrán, M. T., Codella, C., Viti, S., Neri, R., & Cesaroni, R. 2009, ApJ, 690, L93

Bisschop, S. E., Jørgensen, J. K., Bourke, T. L., Bottinelli, S., & van Dishoeck, E. F. 2008, A&A, 488, 959

Blake, G. A., van Dishoek, E. F., Jansen, D. J., Groesbeck, T. D., & Mundy, L. G. 1994, ApJ, 428, 680

Bottinelli, S., et al. 2004, ApJ, 617, L69

Butler, R. A. H., De Lucia, F. C., Petkie, D. T., et al. 2001, ApJS, 134, 319

Carroll, P. B., Drouin, B. J., & Widicus Weaver, S. L. 2010, ApJ, 723, 845

Caux, E., et al. 2011, A&A, 532, A23

Cazaux, S., Tielens, A. G. G. M., Ceccarelli, C., Castets, A., Wakelam, V., Caux, E., Parise, B., & Teyssier, D. 2003, ApJ, 593, L51

Ceccarelli, C., Castets, A., Caux, E., Hollenbach, D., Loinard, L., Molinari, S., & Tielens, A. G. G. M. 2000, A&A, 355, 1129

Chandler, C. J., Brogan, C. L., Shirley, Y. L., & Loinard, L. 2005, ApJ, 632, 371

Crovisier, J., Bockelée-Morvan, D., Biver, N., Colom, P., Despois, D., & Lis, D. C. 2004, A&A, 418, L35

Di Francesco, J., Myers, P. C., Wilner, D. J., Ohashi, N., & Mardones, D. 2001, ApJ, 562, 770

Goldsmith, P. F., Langer, W. D., & Velusamy, T. 1999, ApJ, 519, L173

Halfen, D. T., Apponi, A. J., Woolf, N., Polt, R., & Ziurys, L. M. 2006, ApJ, 639, 237

Herbst, E., & van Dishoeck, E. F. 2009, ARA&A, 47, 427

Hollis, J. M., Jewell, P. R., Lovas, F. J., & Remijan, A. 2004, ApJ, 613, L45

Hollis, J. M., Lovas, F. J., & Jewell, P. R. 2000, ApJ, 540, L107

Hollis, J. M., Lovas, F. J., Jewell, P. R., & Coudert, L. H. 2002, ApJ, 571, L59

Hollis, J. M., Vogel, S. N., Snyder, L. E., Jewell, P. R., & Lovas, F. J. 2001, ApJ, 554, L81

Horn, A., Møllendal, H., Sekiguchi, O., Uggerud, E., Roberts, H., Herbst, E., Viggiano, A. A., & Fridgen, T. D. 2004, ApJ, 611, 605

Jørgensen, J. K., Bourke, T. L., Nguyen Luong, Q., & Takakuwa, S. 2011, A&A, 534, A100

Larralde, R., Robertson, M. P., & Miller, S. L. 1995, Proceedings of the National Academy of Science, 92, 8158

Loinard, L., Torres, R. M., Mioduszewski, A. J., & Rodríguez, L. F. 2008, ApJ, 675, L29

Müller, H. S. P., Thorwirth, S., Roth, D. A., & Winnewisser, G. 2001, A&A, 370, L49

Müller, H. S. P., Schlöder, F., Stutzki, J., & Winnewisser, G. 2005, Journal of Molecular Structure, 742, 215

Öberg, K. I., Garrod, R. T., van Dishoeck, E. F., & Linnartz, H. 2009, A&A, 504, 891

Pickett, H. M., Poynter, I. R. L., Cohen, E. A., Delitsky, M. L., Pearson, J. C., & Muller, H. S. P. 1998, J. Quant. Spec. Radiat. Transf., 60, 883

Pineda, J. E., Maury, A. J., Fuller, G. A., et al. 2012, A&A, in press. (arXiv:1206.5215)

Requena-Torres, M. A., Martín-Pintado, J., Martín, S., & Morris, M. R. 2008, ApJ, 672, 352

Schöier, F. L., Jørgensen, J. K., van Dishoeck, E. F., & Blake, G. A. 2002, A&A, 390, 1001

Schöier, F. L., Jørgensen, J. K., van Dishoeck, E. F., & Blake, G. A. 2004, A&A, 418, 185

van Dishoeck, E. F., Blake, G. A., Jansen, D. J., & Groesbeck, T. D. 1995, ApJ, 447, 760

Widicus Weaver, S. L., Butler, R. A. H., Drouin, B. J., et al. 2005, ApJS, 158, 188

Wilson, T. L., & Rood, R. 1994, ARA&A, 32, 191

Woods, P. M., Kelly, G., Viti, S., Slater, B., Brown, W. A., Puletti, F., Burke, D. J., & Raza, Z. 2012, ApJ, 750, 19

Wootten, A. 1989, ApJ, 337, 858

Yeh, S. C. C., Hirano, N., Bourke, T. L., Ho, P. T. P., Lee, C., Ohashi, N., & Takakuwa, S. 2008, ApJ, 675, 454

Table 2: Results of the model fits to the methyl formate and glycolaldehyde.

	I16293A	I16293B
Temperature	200 K	300 K
N_{60AU}(Methyl formate)	5×10^{17} cm^{-2}	4×10^{17} cm^{-2}
N_{60AU}(Glycolaldehyde)	4×10^{16} cm^{-2}	3×10^{16} cm^{-2}